

**Dynamic-Pressure Measurements  
Using an Electronically  
Scanned Pressure Module**

**FOR REFERENCE**

NOT TO BE TAKEN FROM THIS ROOM

William G. Chapin

JULY 1983

**LIBRARY COPY**

JUL 20 1983

LANGLEY RESEARCH CENTER  
LIBRARY AREA  
HAMPTON, VIRGINIA



25th Anniversary  
1958-1983

**NASA**



NASA Technical Memorandum 84650

**Dynamic-Pressure Measurements  
Using an Electronically  
Scanned Pressure Module**

**William G. Chapin**  
*Langley Research Center*  
*Hampton, Virginia*



National Aeronautics  
and Space Administration

**Scientific and Technical  
Information Branch**

1983



## SUMMARY

Amplitude and phase responses were measured for different lengths and diameters of tubing between a sinusoidal-pressure source and a pressure-sensing module from an electronically scanned pressure-measuring system. Measurements were made for straight runs of both steel and vinyl tubing. For steel tubing, measured results are compared with results calculated by using equations developed by Tijdeman and Bergh. Measurements were also made with a bend in the vinyl tubing at the module. In addition, measurements were made with two coils placed in the tubing near the middle of the run. All data were obtained at atmospheric pressure with a temperature of 297 K (75°F).

For the lengths and diameters tested, the sinusoidal response was satisfactory at frequencies less than 15 Hz. The agreement between the theoretical and experimental results is good enough to make the Tijdeman-Bergh equations a useful design tool. For straight tubing, the difference in sinusoidal response between steel and vinyl tubing is not significant for most applications.

## INTRODUCTION

Over the past several years at the Langley Research Center, considerable effort has been devoted to developing electronically scanned pressure (ESP) systems for making steady-state, multichannel pressure measurements. A typical ESP system contains the following components: a multichannel pressure-sensor module which houses a separate transducer for each channel; tubing connecting each channel to its source of pressure; and electronic and pneumatic equipment for performing in situ calibrations and for sequentially measuring the pressure applied to each channel. A typical multichannel module has a rectangular volume of 66 cm<sup>3</sup> (4 in<sup>3</sup>) and contains 32 individual silicon-diaphragm, piezoresistive pressure transducers. The negative side of each transducer is connected to a common reference pressure port. The module also contains an amplifier and circuitry for multiplexing the analog outputs of the transducers.

Considerable cost savings in equipment can be obtained by using such an ESP system as opposed to a system having, for each channel of data, an individual transducer with separate signal-conditioning equipment. Moreover, the installation process is simplified because an ESP system has fewer electrical leads. Furthermore, sampling-rate limitations due to pneumatic settling times are eliminated by use of an ESP system instead of the type of sampled-data system in which a single transducer is sequentially connected to each pressure source by a mechanical-type pressure-sampling valve. Moreover, because of its relatively small size and the fact that its rectangular shape simplifies mounting, an ESP system module can often be placed closer to pressure sources than a mechanical-type valve.

Because of these advantages, the possibility of adapting the ESP concept for multichannel dynamic-pressure measurements is being investigated theoretically and experimentally. Essentially, equipment would have to be designed to interface the ESP system to a computer. The geometry of the ESP module would remain essentially unchanged. A particular application would be to measure dynamic pressures resulting from the sinusoidal oscillation of airfoils at frequencies as high as 30 Hz. An

important consideration, of course, is the effect of the tubing between the module and the pressure source on the dynamic response of the system. Therefore, the sinusoidal amplitude and phase responses were measured for different lengths and diameters of tubing between a pressure source and one channel of the ESP module. This report describes the procedures used for making these measurements and the results obtained. Furthermore, measured results are compared with theoretical calculations from equations developed by Tijdeman and Bergh. (See refs. 1 and 2.)

#### SYMBOLS

Values are given in SI units and, where considered useful, also in U.S. units. Measurements and calculations were made in U.S. Customary Units.

$\text{bei}(x)$	imaginary part of $J_0(i^{3/2}x)$
$\text{bei}_2(x)$	imaginary part of $J_2(i^{3/2}x)$
$\text{ber}(x)$	real part of $J_0(i^{3/2}x)$
$\text{ber}_2(x)$	real part of $J_2(i^{3/2}x)$
$c_p$	specific heat at constant pressure
$c_v$	specific heat at constant volume
$d_j$	diameter of tube $j$
$f$	frequency of sinusoidal fluctuation
$i$	$= \sqrt{-1}$
$J_0(x)$	zero-order Bessel function of argument $x$
$J_2(x)$	second-order Bessel function of argument $x$
$L_j$	length of tube $j$
$n_j$	parameter of tube $j$ as defined in equation (A4)
$P_i, P_j, P_t$	complex variables representing sinusoidal pressure fluctuations at tubing-system inlet, end of tube $j$ , and transducer, respectively
$P_o$	average pressure
$s_j$	parameter of tube $j$ as defined in equation (A5)
$U_o$	average velocity parallel to entrance of tube 1 (see fig. A1)
$V_j$	volume of cavity between tube $j$ and tube $j+1$
$x$	dummy variable
$(\alpha + i\beta)_j$	complex parameter of tube $j$ as defined in equation (A3)

$\gamma$	$= c_p/c_v$
$\mu$	viscosity
$\rho_o$	average density
$\sigma$	square root of Prandtl number
$\omega$	$= 2\pi f$

#### Abbreviations:

ESP	electronically scanned pressure
i.d.	inside diameter

### EXPERIMENTAL APPARATUS AND PROCEDURE

This section describes the experimental apparatus and those aspects of the experimental procedure common to all tests conducted. Additional details that pertain only to a specific test are contained in the section describing that test. A block diagram of the experimental setup is shown in figure 1, and a photograph is shown in figure 2. The sinusoidal-pressure generator, ESP module, and connecting tube are shown in greater detail in figure 3. With this apparatus, the amplitude ratio  $|p_t/p_i|$  and the phase shift  $\angle p_t/p_i$  were determined. As shown in figures A1 and A2 of the appendix,  $p_i$  is a complex variable representing the sinusoidal-pressure fluctuation about an average pressure  $p_o$  at the tube inlet, and  $p_t$  is a complex variable representing the resulting pressure fluctuation at the transducer in the ESP module. In all tests,  $p_o$  was atmospheric pressure. As also illustrated in figure 3, the sinusoidal pressure of about 6000 Pa (0.9 psi) at the tube inlet was generated in the cylinder of the sinusoidal-pressure generator by means of an oscillating piston which was driven by an electric motor. The pressure was measured by the reference transducer which was flush mounted at the cylinder head of the sinusoidal-pressure generator. This transducer was a flush-diaphragm, strain-gage-type differential-pressure transducer.

The outlet of the connecting tube was connected to 1 channel of a 32-channel ESP module. To obtain a continuous output signal from that one channel, the electronic switching circuitry in the module was bypassed. As shown in figure 3, the internal tubing of the module was part of the overall tube-transducer system. As shown in figure 1, the electrical output of the reference transducer was connected to channel A of the gain-and-phase meter. The output of the ESP module transducer was connected to channel B. This phase-and-gain meter displayed both the phase difference between the signals at channels A and B and the ratio of the magnitude of the signal at channel B to that at channel A. To enable the phase-and-gain meter to display directly the amplitude ratio  $|p_t/p_i|$ , the ESP module transducer used in the tests was first statically calibrated. Then, the gain of the variable-gain amplifier was adjusted so that the calibration factor of the reference-transducer—variable-gain amplifier combination equaled that of the module transducer. The sinusoidal frequency was measured with the frequency meter which was connected to the output of the variable-gain amplifier. Bridge voltages for the reference transducer and for the ESP module transducer were furnished by dc power-supply no. 1 and dc power-supply no. 2, respectively. The dual dc power supply furnished power for the other module electronics. The signals from the reference transducer and the ESP module transducer

were monitored with the dual-beam oscilloscope. The voltmeter, shown in figure 1 as monitoring the output of the variable-gain amplifier, was also used as needed to set the various power-supply voltages and to monitor the voltage output of the ESP transducer.

## RESULTS

By using steel tubing connected between the sinusoidal-pressure generator and the ESP module, the sinusoidal response was determined by using the procedures and experimental setup described in the preceding section. Measurements were made for 0.1-cm (0.039-in.) i.d. tubing at lengths of 34 cm (13.5 in.), 61 cm (24 in.), and 76 cm (30 in.) and for 0.15-cm (0.06-in.) i.d. tubing at lengths of 61 and 76 cm. The results are shown in figures 4 and 5. As shown in figure 3, the foregoing lengths are those from the end of the cylinder of the sinusoidal-pressure generator to the connecting tube of the ESP module. The calculated-response curves were obtained by the procedure described in the appendix. A value of 0.1 cm was used for the diameter  $d$  to obtain the calculated results shown. (See fig. 4.) It is conceivable that the diameter could vary along the length of the tube and that the cross section could be noncircular in some places. Consequently, the effective value of the tube diameter could differ from the nominal value. Therefore, to account possibly for the difference between the experimental and calculated results, the response for the tubing lengths of 61 and 76 cm was also calculated for diameters less than 0.1 cm. The results for the 61- and 76-cm lengths of tubing are shown in figures 6 and 7, respectively, and the experimental data shown in figure 4 are also shown in these figures.

The values used to obtain the calculated results are as follows:

$$p_o = 0.1014 \text{ MPa (2117 psf)}$$

$$\gamma = 1.4$$

$$\mu = 18 \text{ } \mu\text{N-sec/m}^2 \text{ (} 3.8 \times 10^{-7} \text{ lb-sec/ft}^2 \text{)}$$

$$\rho_o = 1.190 \text{ kg/m}^3 \text{ (} 2.309 \times 10^{-3} \text{ slug/ft}^3 \text{)}$$

$$\sigma = 0.8774$$

The preceding value of viscosity  $\mu$  is for air at 297 K (75°F). This temperature was used to calculate the average density  $\rho_o$  from the ideal-gas law. The values used for the lengths and diameters of the internal tubing of the ESP module are shown in figure 3.

In many pressure-measuring systems, vinyl tubing is used rather than metal tubing. The use of vinyl tubing, of course, introduces the cross-sectional elasticity of the tubing as an additional factor which could conceivably affect the dynamic response. Therefore, sinusoidal-response measurements were made with 0.09-cm (0.035-in.) i.d. polyvinyl-chloride plastic tubing connected between the sinusoidal-pressure generator and the ESP system module. It would, of course, have been



desirable to use plastic tubing with an inside diameter of 0.1 cm (0.039 in.), which would have corresponded to a diameter used in some of the steel-tubing tests.

The sinusoidal response was determined for a straight run of tubing at lengths of 61 and 76 cm (24 and 30 in.). As shown in figure 8(a), the length L included a section of 0.1-cm (0.039-in.) i.d. steel tubing that was 6.4 cm (2.5 in.) long, which coupled the vinyl tubing to the sinusoidal generator. The dynamic response was also determined for the situation in which the 61-cm-long tubing was bent at the module, as shown in figure 8(b). Tests were performed for bend radii of approximately 5 and 13 cm (2 and 5 in.). In addition, the dynamic response was determined for the situation in which the 61-cm-long tubing was coiled in two places near the middle of the tube, as shown in figure 8(c). The diameter of each coil was approximately 5 cm (2 in.). Bending or coiling the tubing was carefully done to avoid constrictions.

The results of each test performed with the 61-cm-long (24-in.) tubing are shown in figure 9, which also shows the results from figure 4 for the 0.1-cm (0.039-in.) i.d. steel tubing that was 61 cm long. The results of the measurements made for the 76-cm-long (30-in.) tubing are shown in figure 10, which also shows the results from figure 4.

#### DISCUSSION

In general, the tube lengths and diameters tested are typical of those used in actual pressure-measurement systems involving ESP modules. For these lengths and diameters, the sinusoidal response, in most instances, will be satisfactory for frequencies less than 15 Hz. At higher frequencies, it appears that a satisfactory dynamic-response characteristic can be obtained for some applications by a careful choice of tube length and diameter. By extrapolating the results shown in figure 4, one can conclude that, generally, the best response can be obtained by making the tube length as short as possible. This conclusion is, of course, consistent with that derived from practical experience by many persons in the dynamic-pressure-measurement field. However, in many situations, one is constrained to a minimum allowable tube length. In these situations, trade-offs often need to be made. For example, as shown in figure 4, increasing the tube length from 61 to 76 cm (24 to 30 in.) resulted in a flatter amplitude response but, at the same time, larger phase lags. As another example, increasing the tube inside diameter resulted in degraded amplitude responses but smaller phase lags. (See figs. 4 and 5.) Another trade-off situation arises from the fact that the sinusoidal response depends, among other things, on the average pressure, average density, and average temperature. (See eqs. (A1) to (A5).) Therefore, an optimum tubulation system at one set of thermodynamic conditions can be less than optimum at another set.

There is reasonably good agreement between experimental and calculated results except near the maximum values of the amplitude-response characteristic for the 0.1-cm (0.039-in.) i.d. tubing. (See fig. 4.) It is uncertain whether the discrepancies result primarily from imperfections in the Tijdeman-Bergh mathematical model or from differences between the actual inside diameter and the 0.1-cm nominal value used in calculating the results. For example, the results (fig. 6) suggest that the effective diameter of the 61-cm (24-in.) length of tubing could actually have been 7 to 9 percent less than the assumed value of 0.1 cm and that the effective inside diameter of the 76-cm (30-in.) length of tubing could have been about 10 to 12 percent less (fig. 7) than the assumed value. These possibilities do not seem unreasonable for tubing having a 0.1-cm inside diameter. This would account for these amplitude-response discrepancies. However, it was outside the scope of these tests

to investigate this question in more detail. In spite of the uncertainty, however, the Tijdeman-Bergh mathematical model appears to be a useful design tool.

When a straight run of vinyl tubing was substituted for the steel tubing, the resulting change in amplitude response was insignificant for most applications. (See figs. 9 and 10.) When the plastic tube was bent at the module, a small improvement in amplitude response resulted. When the tube was coiled, a significant flattening of the amplitude response occurred. These data suggest that it might be feasible to control the sinusoidal response by coiling the tubing. For most applications, the change in phase lags resulting from substituting plastic tubing for steel tubing (figs. 9 and 10) would not be significant.

#### CONCLUSIONS

From the results of this theoretical and experimental investigation on the sinusoidal response of a system consisting of tubing and an electronically scanned pressure module, the following conclusions are presented:

1. For 0.1- and 0.15-cm (0.039- and 0.06-in.) inside-diameter tubing of lengths less than 76 cm (30 in.), the sinusoidal response, in most instances, is satisfactory for frequencies less than 15 Hz.
2. The Tijdeman-Bergh mathematical model is useful in the design of the transducer-tubulation system.
3. The difference in sinusoidal response between a straight run of steel tubing and a straight run of vinyl tubing is insignificant for most applications.
4. Coiling the tubing shows promise as a method of improving the sinusoidal response and should be investigated further.

Langley Research Center  
National Aeronautics and Space Administration  
Hampton, VA 23665  
May 17, 1983

## APPENDIX

### TIJDEMAN-BERGH SINUSOIDAL-RESPONSE EQUATIONS

This appendix contains a brief discussion of the theoretical work done by Tijdeman and Bergh on the dynamic response of pressure-measuring systems. (See refs. 1 and 2.) First, the theory pertaining to the general tube-transducer system shown in figure A1 is discussed. Then, the specialization of this theory to the tube-transducer system tested is discussed. Finally, the method for obtaining the calculated results presented in this paper is discussed.

In reference 1, Tijdeman derived recursion formulas from which the dynamic response of the tube-transducer system of figure A1 can be calculated. His work was based on the earlier work described in reference 2. One recursion formula is given by equation (B.47) of reference 1. Because the equation is long and involved, it is not being explicitly stated. It expresses the complex ratio  $p_j/p_{j-1}$  in terms of  $p_{j+1}/p_j$ , the volume  $V_j$ , the lengths and diameters of tubes  $j$  and  $j+1$ , and the following environmental parameters: viscosity, average density, average pressure, the square root of the Prandtl number, and the ratio of the specific heat at constant pressure to that at constant volume. However, for tube  $N$ , which is just ahead of the transducer, terms involving  $p_{j+1}$  and the dimensions of the tube  $j+1$  vanish. Equation (B.47) applies when  $j = N, N - 1, \dots, 3, 2$ , but it does not apply when  $j = 1$ . For  $j = 1$ , that is, for tube 1, Tijdeman (ref. 1) found that the recursion relation between  $p_1/p_i$  and  $p_2/p_1$  depends on  $U_0$ , the average velocity parallel to the entrance to tube 1, in addition to the factors contained in equation (B.47). This recursion relationship for  $j = 1$  is expressed by equation (B.51) of reference 1. When  $U_0 = 0$ , equation (B.51) reduces to equation (B.47).

Equations (B.47) and (B.51) from reference 1 are derived from the Navier-Stokes equations, the energy equation, and the equation of state for an ideal gas. It is assumed that the sinusoidal-pressure fluctuations are small enough to allow second-order perturbation terms to be neglected. Furthermore, it is assumed that the pressure fluctuations are equal at the exit from tube  $j$ , in the cavity volume  $V_j$ , and at the entrance to tube  $j+1$ . As an important special case, the pressure fluctuation at the sensing element of the pressure transducer and at the exit from tube  $N$  are assumed to be equal. The volume  $V_N$  could be a cavity volume external to a flush diaphragm transducer, part of the internal volume of a transducer, or a combination of internal and external volumes. (See fig. A1.) To compute the sinusoidal response  $p_t/p_i$ , first, the response  $p_j/p_{j-1}$  is computed for each tube by starting with tube  $N$  and working from right to left. As mentioned earlier, equation (B.47) is used for  $j = N, N - 1, \dots, 3, 2$ , and equation (B.51) is used for  $j = 1$ . The end result,  $p_t/p_i$ , is then obtained by multiplying the preceding responses.

The tube-transducer system consisting of the external tubing and ESP system module is somewhat simpler than the general system shown in figure A1. As shown in figure 3, the external tubing plus the internal tubing of the ESP module comprises a three-tube system with no intermediate cavity volumes. Furthermore, in the ESP system module, there is negligible cavity volume ahead of a transducer. Consequently, the configuration shown in figure A1 simplifies to the three-tube zero-volume configuration shown in figure A2. The fact that  $U_0 = 0$  further simplifies the situation.

APPENDIX

As a result of the preceding simplifications, the recursion equation (B.47) of reference 1 reduces for  $j = 2$  to

$$\frac{p_j}{p_{j-1}} = \left\{ \cosh (\alpha + i\beta)_j + \frac{d_{j+1}^2 L_{j+1} n_j (\alpha + i\beta)_j \sinh (\alpha + i\beta)_j}{d_j^2 L_j n_{j+1} (\alpha + i\beta)_{j+1} \sinh (\alpha + i\beta)_{j+1}} \right. \\ \left. \times \left[ \cosh (\alpha + i\beta)_{j+1} - \frac{p_{j+1}}{p_j} \right] \right\}^{-1} \quad (A1)$$

Since  $U_0 = 0$ , the preceding equation also applies when  $j = 1$ . For  $j = 1$ ,  $p_{j-1} = p_i$  by definition, and for  $j = 3$ , terms with the subscript  $j+1$  vanish. Consequently, for  $j = 3$ ,

$$\frac{p_j}{p_{j-1}} = \frac{p_3}{p_2} = \frac{p_t}{p_2} = \left[ \cosh (\alpha + i\beta)_3 \right]^{-1} \quad (A2)$$

The parameters appearing in equations (A1) and (A2) are as follows:

$$(\alpha + i\beta)_j = \frac{L_j \rho_o^{1/2} \omega}{p_o^{1/2}} \left[ \frac{\text{ber}(s_j) + i \text{bei}(s_j)}{\text{ber}_2(s_j) + i \text{bei}_2(s_j)} \frac{1}{n_j} \right]^{1/2} \quad (A3)$$

$$n_j = \left[ 1 + \frac{\gamma - 1}{\gamma} \frac{\text{ber}_2(\sigma s_j) + i \text{bei}_2(\sigma s_j)}{\text{ber}(\sigma s_j) + i \text{bei}(\sigma s_j)} \right]^{-1} \quad (A4)$$

$$s_j = \frac{d_j}{2} \left( \frac{\rho_o \omega}{\mu} \right)^{1/2} \quad (A5)$$

Equation (A3) is the result of multiplying a modified version of equation (5.1a) of reference 1 by  $\omega L_j$ . Equation (A4) is a modified version of equation (5.1b) of

APPENDIX

reference 1, and equation (A5) is equivalent to equation (5.1c) of reference 1. In equations (A3) and (A4),

$$\text{ber}(x) + i \text{bei}(x) = J_0(i^{3/2}x)$$

where  $x$  is a dummy variable representing  $s$  or  $\sigma s$ .

The sinusoidal response  $p_t/p_i$  is calculated by first determining  $p_t/p_2$  by use of equations (A2) to (A5). Then, for  $j = 2$  and  $j = 1$ ,  $p_2/p_1$  and  $p_1/p_i$  are determined by using equations (A1) and (A3) to (A5). Finally,  $p_t/p_i$  is obtained by multiplying the responses of the individual tubes. That is,

$$\frac{p_t}{p_i} = \frac{p_t}{p_2} \frac{p_2}{p_1} \frac{p_1}{p_i} \tag{A6}$$

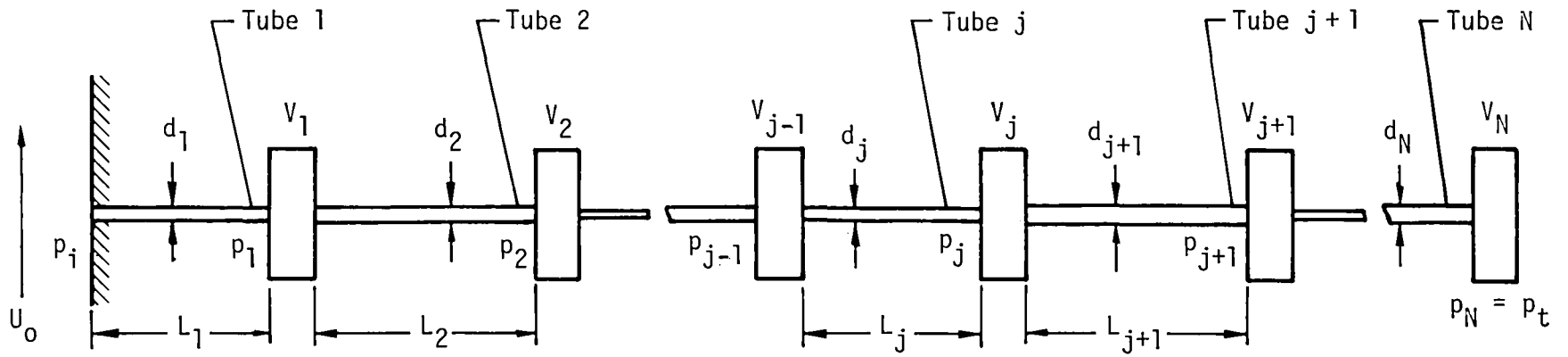


Figure A1.- Generalized tubulation-transducer system.

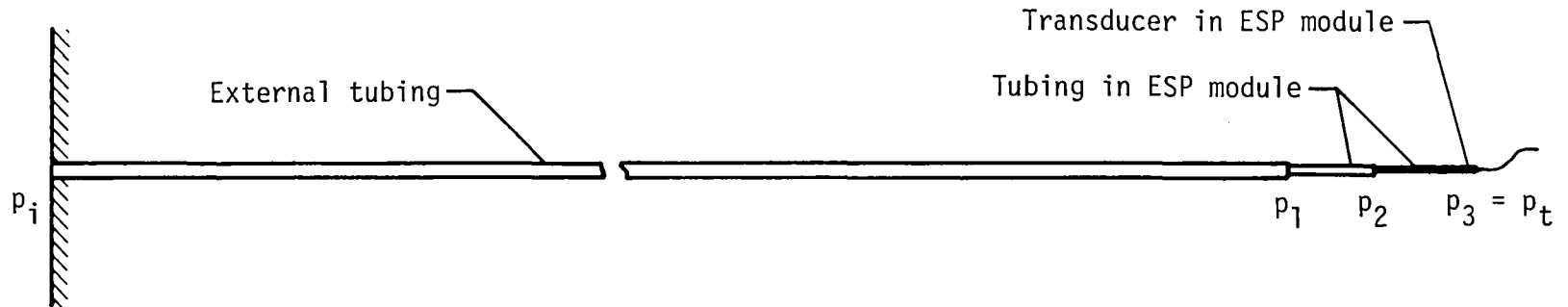


Figure A2.- Specialized tubulation-transducer system consisting of external tubing and ESP internal tubing and transducer.

#### REFERENCES

1. Tijdeman, H.: Investigations of the Transonic Flow Around Oscillating Airfoils. Rep. NLR-TR-77090 U, Nat. Luchtvaartlab. (Amsterdam), 1977. (Available from DTIC as AD B027 633.)
2. Bergh, H.; and Tijdeman, H.: Theoretical and Experimental Results for the Dynamic Response of Pressure Measuring Systems. Rep. NLR-TR F.238, Nat. Luchtvaartlab. (Amsterdam), Jan. 1965.

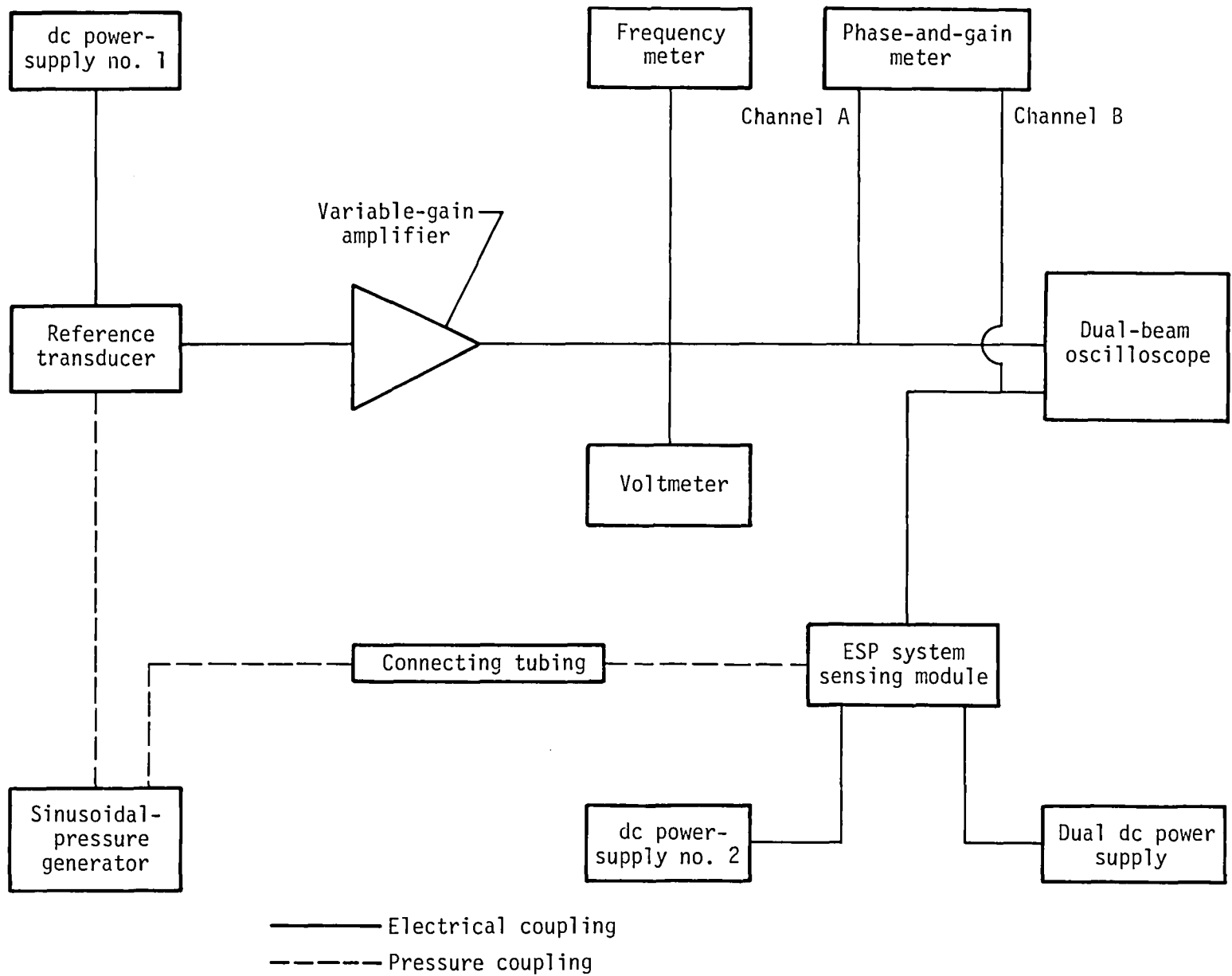
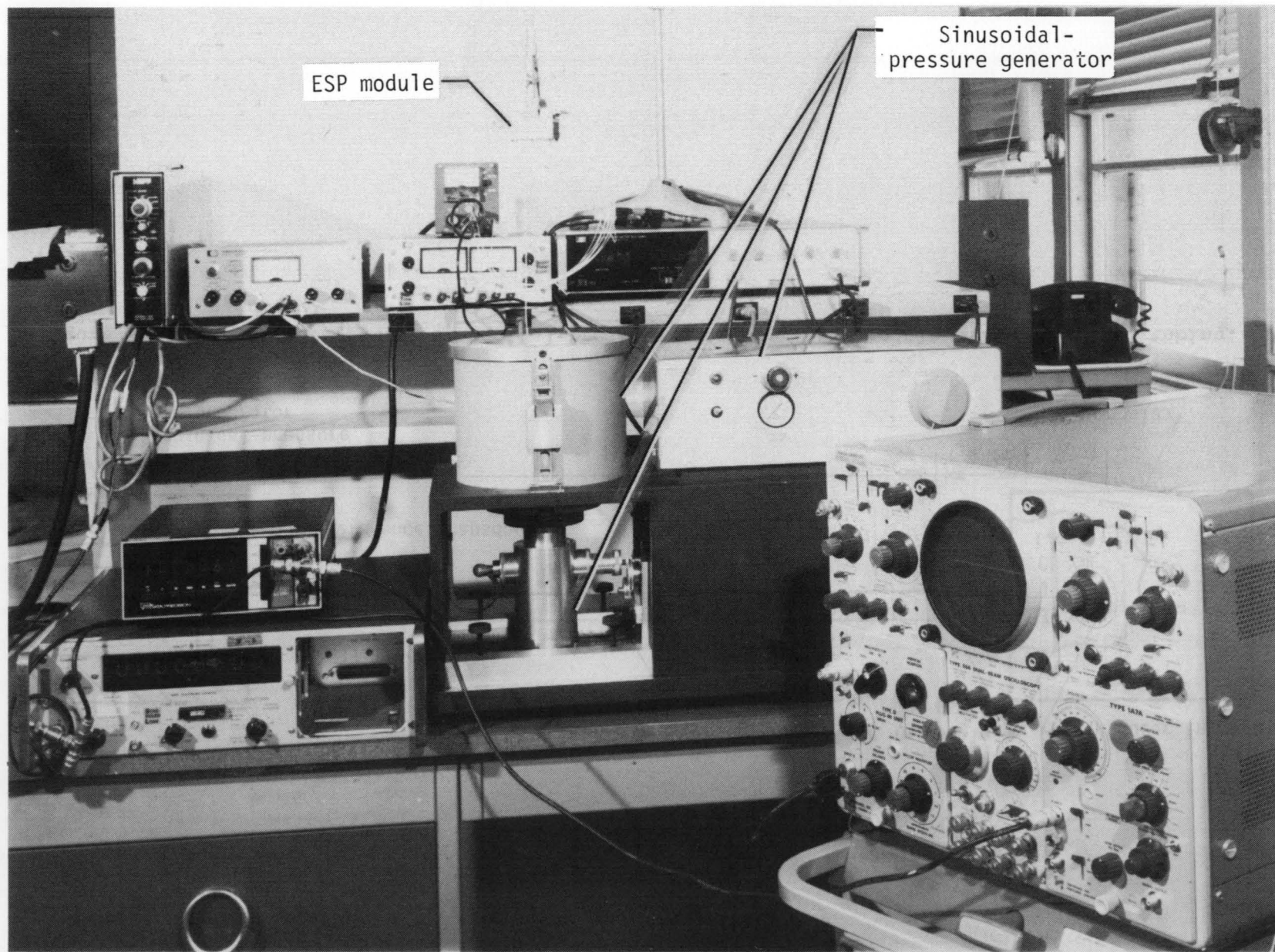


Figure 1.- Block diagram of apparatus for sinusoidal-response measurements of ESP module.





ESP module

Sinusoidal-pressure generator

L-83-88

Figure 2.- Apparatus for sinusoidal-response measurements of ESP module.

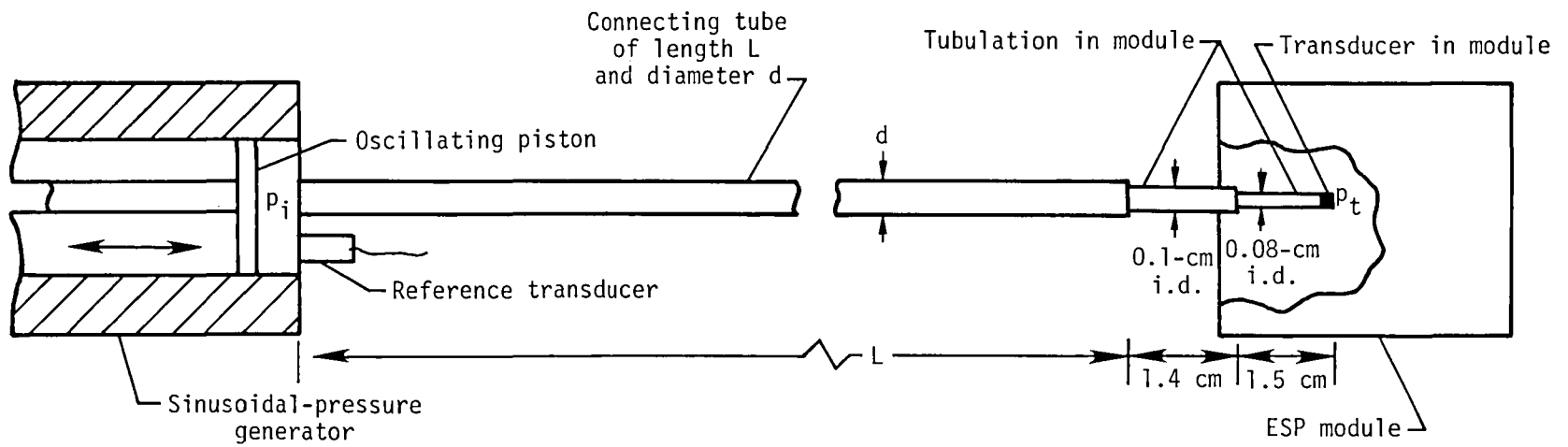


Figure 3.- Schematic diagram of sinusoidal-pressure generator, ESP module, and connecting tubing.

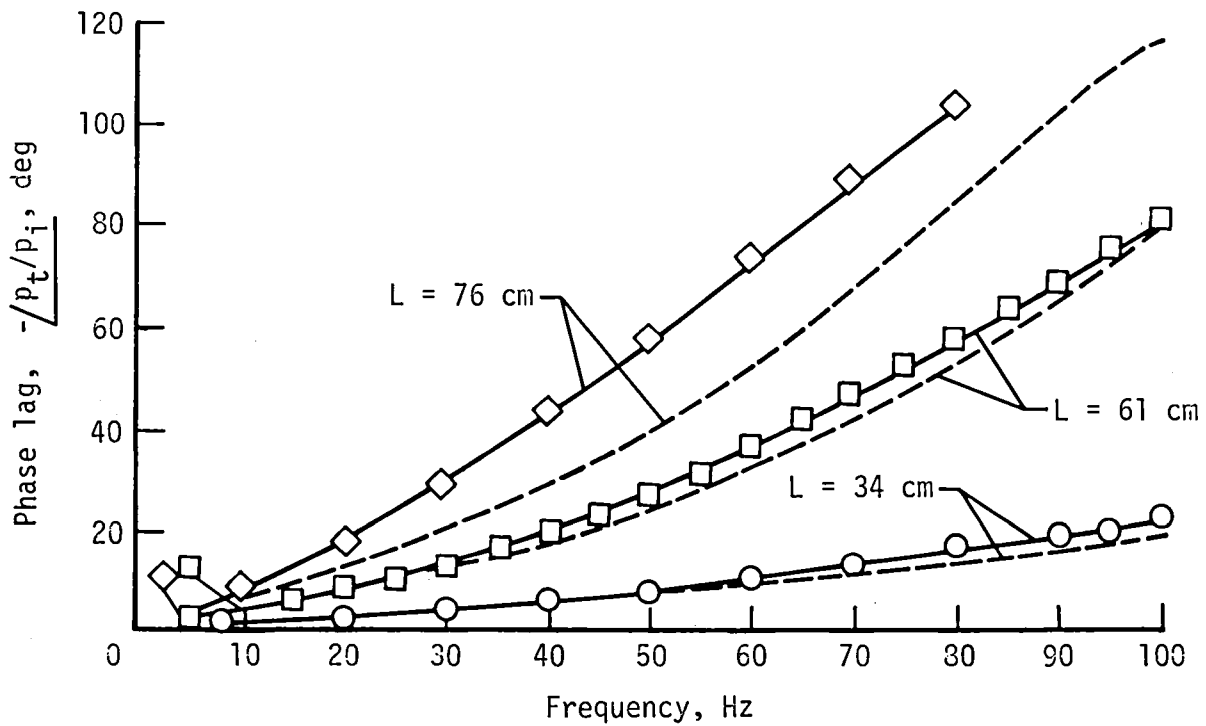
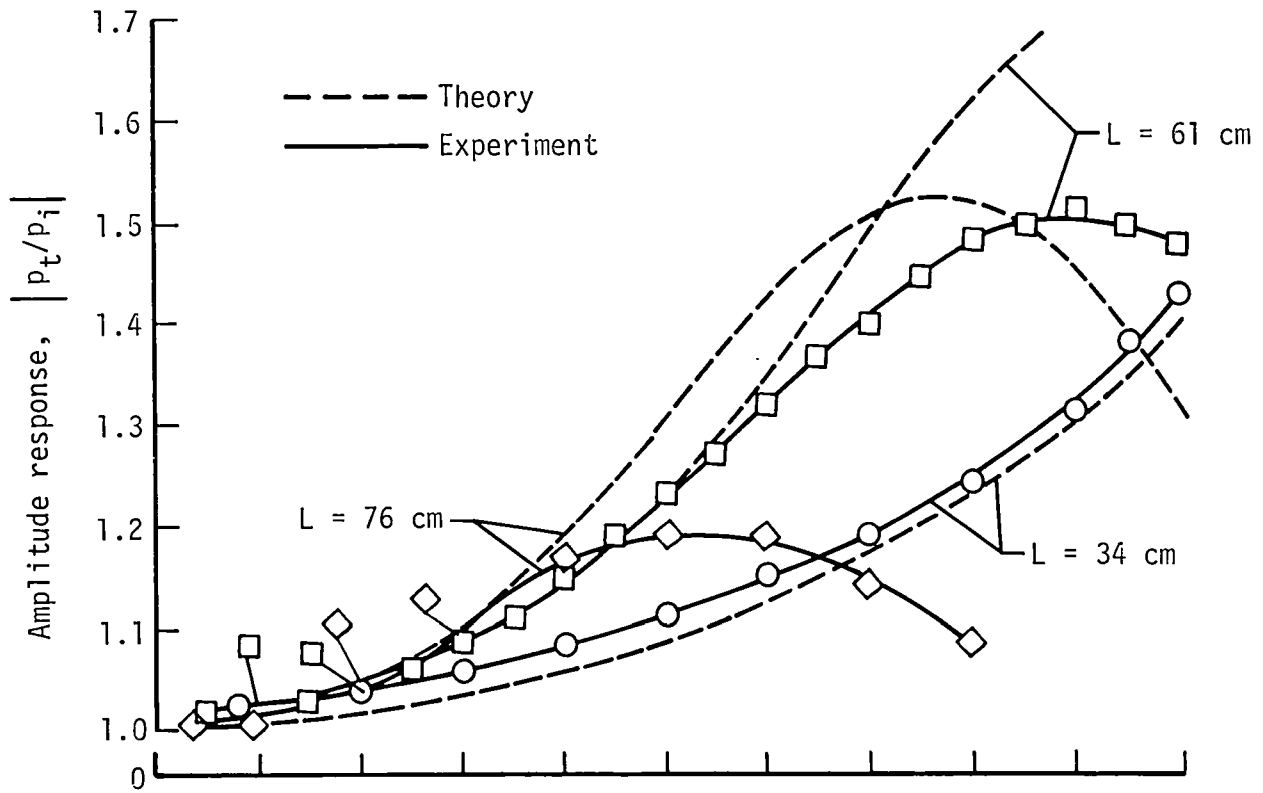


Figure 4.- Sinusoidal response for 0.1-cm inside-diameter steel tubing.

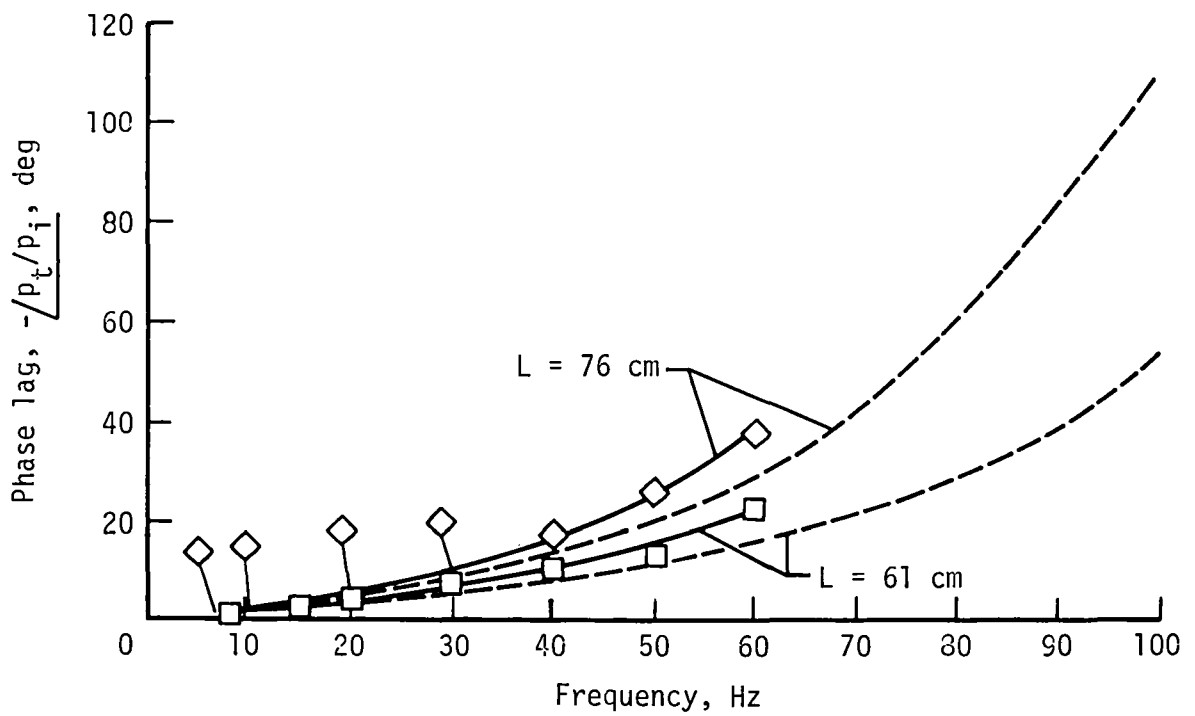
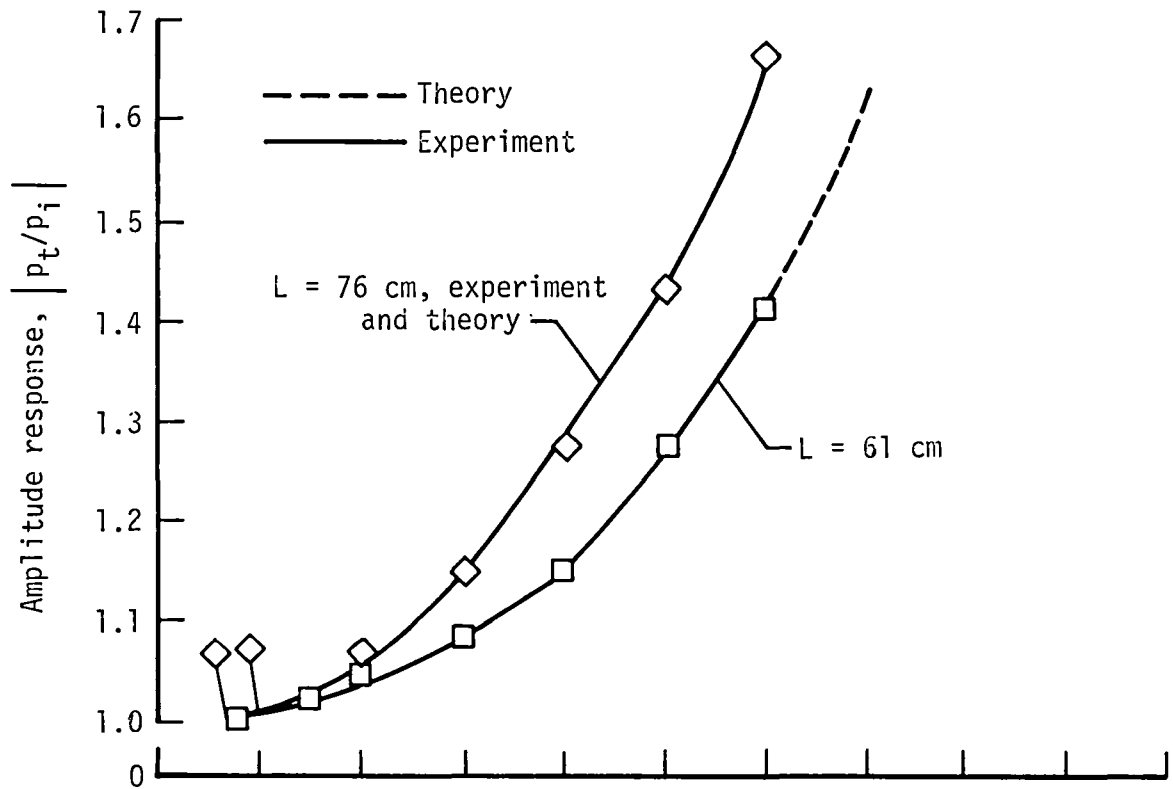


Figure 5.- Sinusoidal response for 0.15-cm inside-diameter steel tubing.

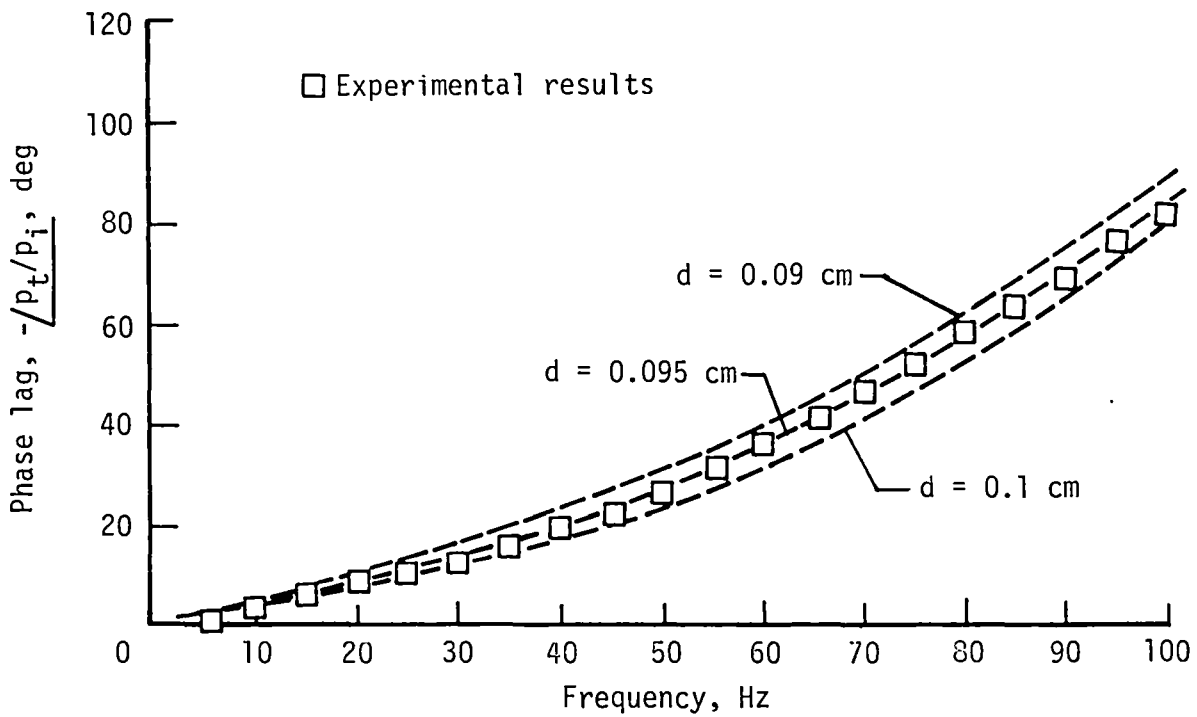
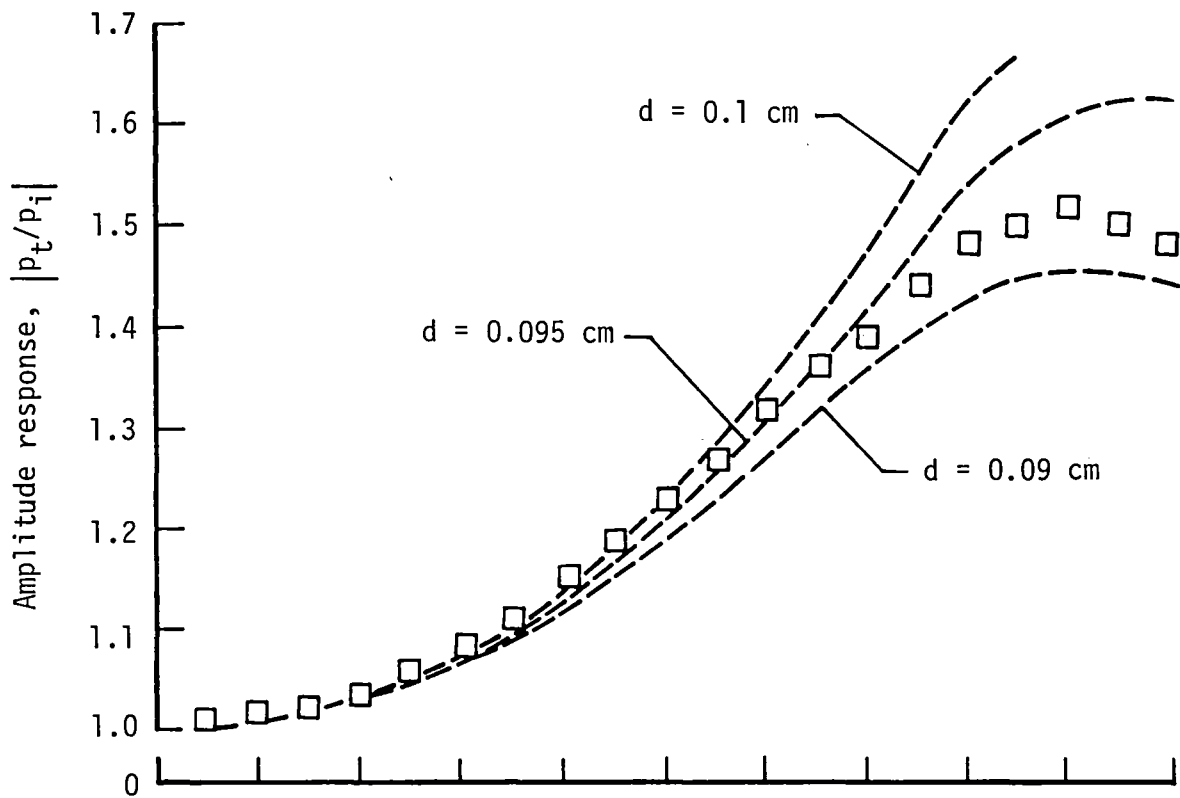


Figure 6.- Sensitivity of calculated sinusoidal response to small changes in diameter for 61-cm tube length.

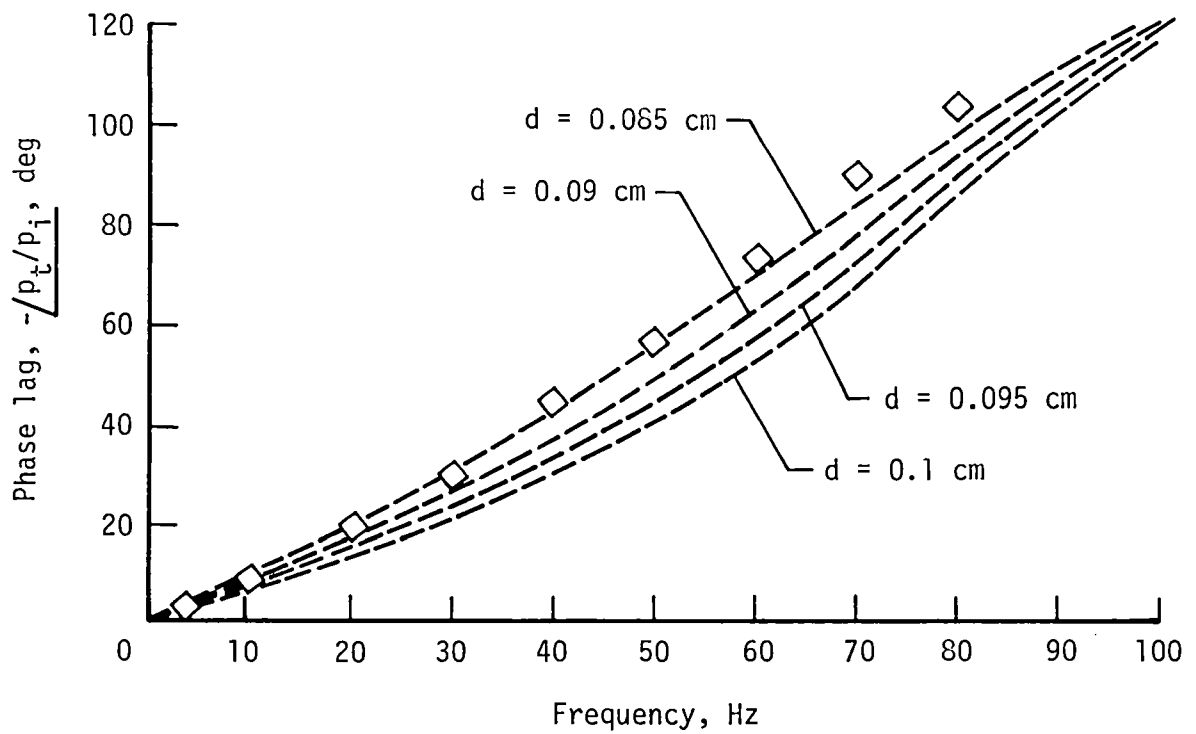
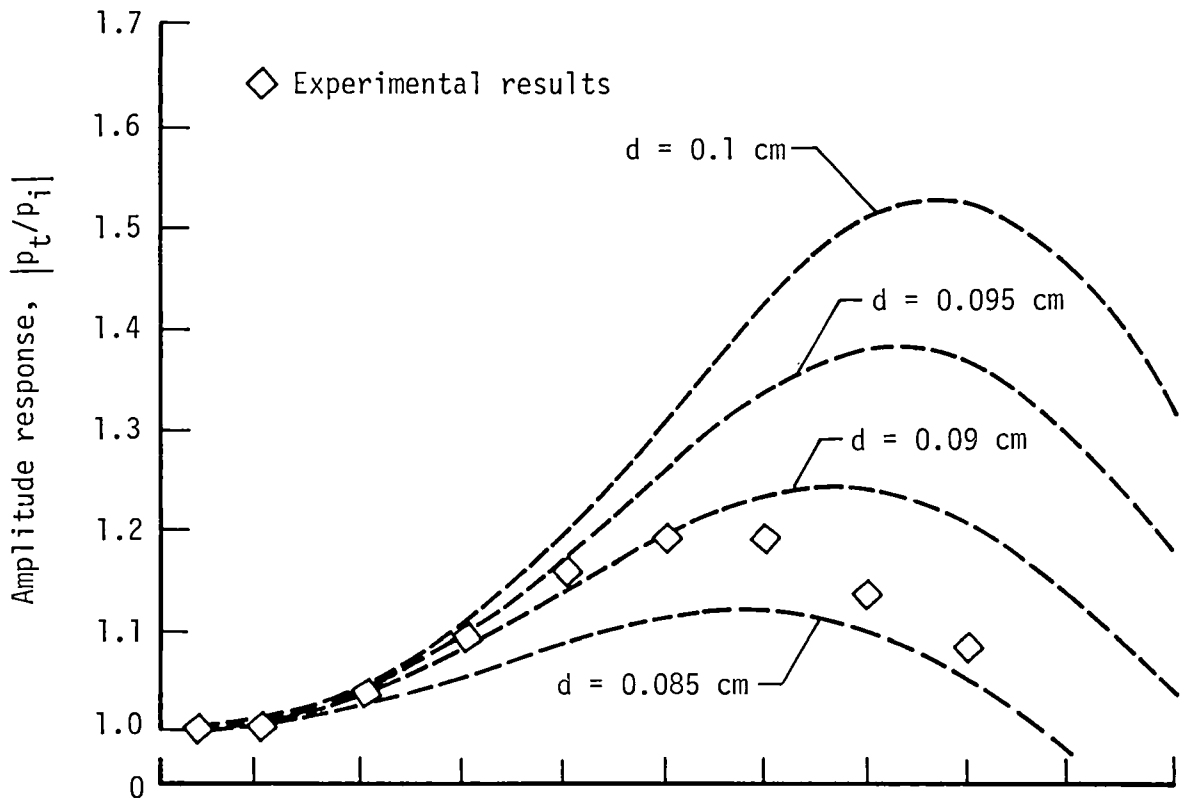
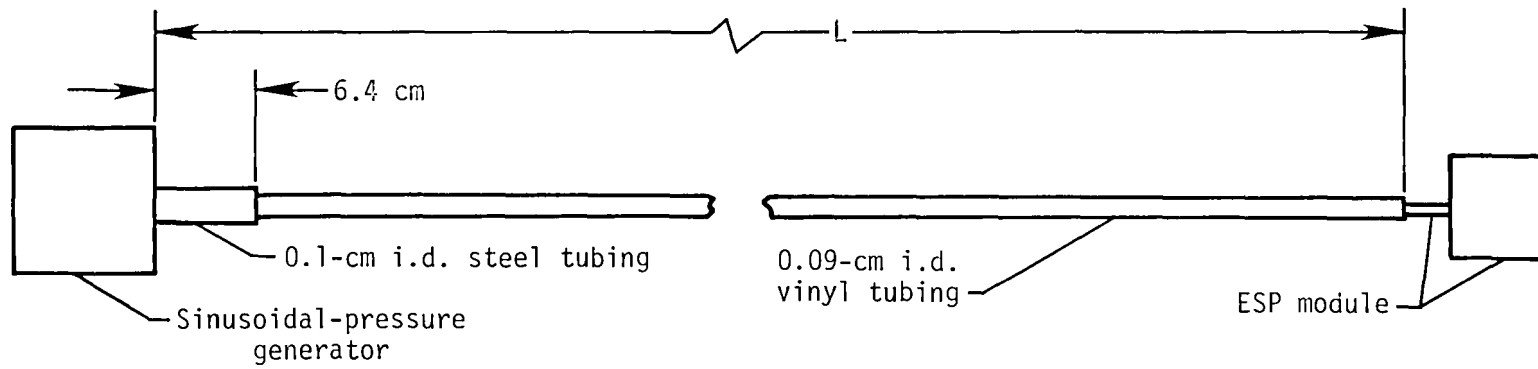
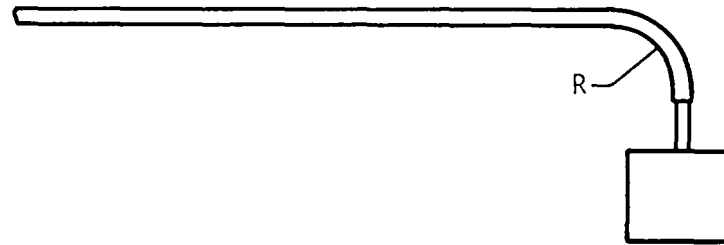


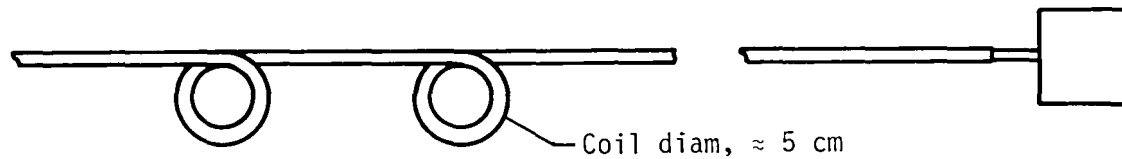
Figure 7.- Sensitivity of calculated sinusoidal response to small changes in diameter for 76-cm tube length.



(a) Straight run of tubing.



(b) Bend of radius  $R$  at module  $R$ .  $R = 5$  and  $13$  cm.



(c) Two coils near center of tubing run.

Figure 8.- Schematic diagrams giving summary of tests using vinyl tubing.

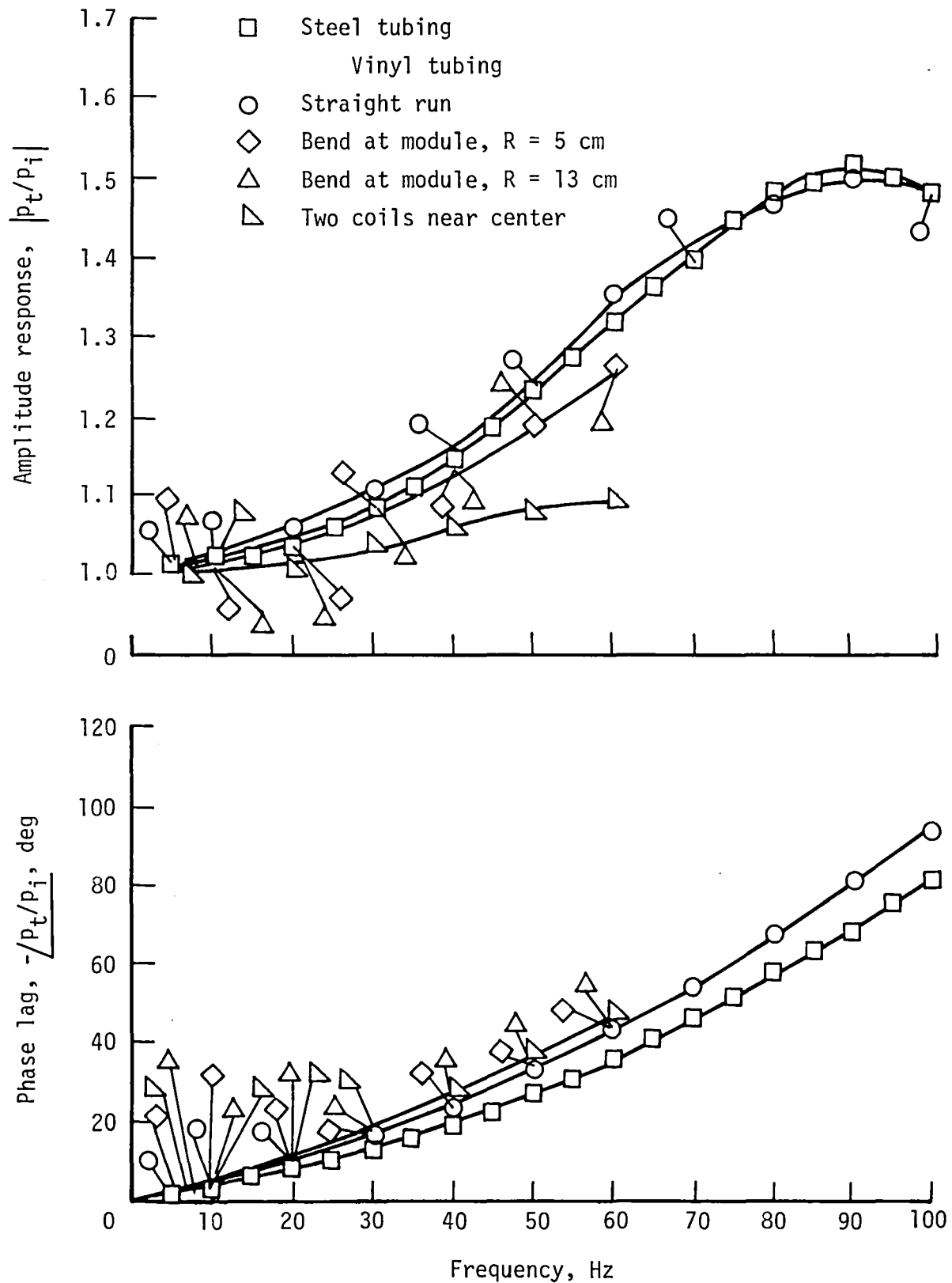


Figure 9.- Sinusoidal response for 0.09-cm inside-diameter vinyl tubing that was 61 cm long.



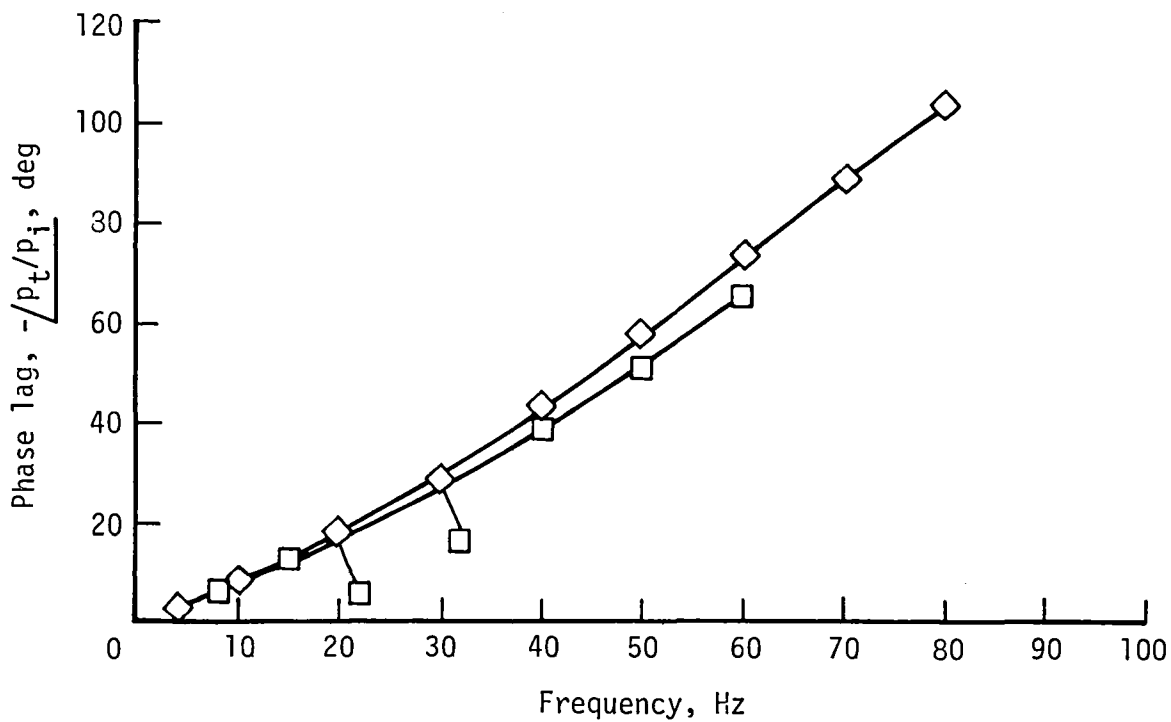
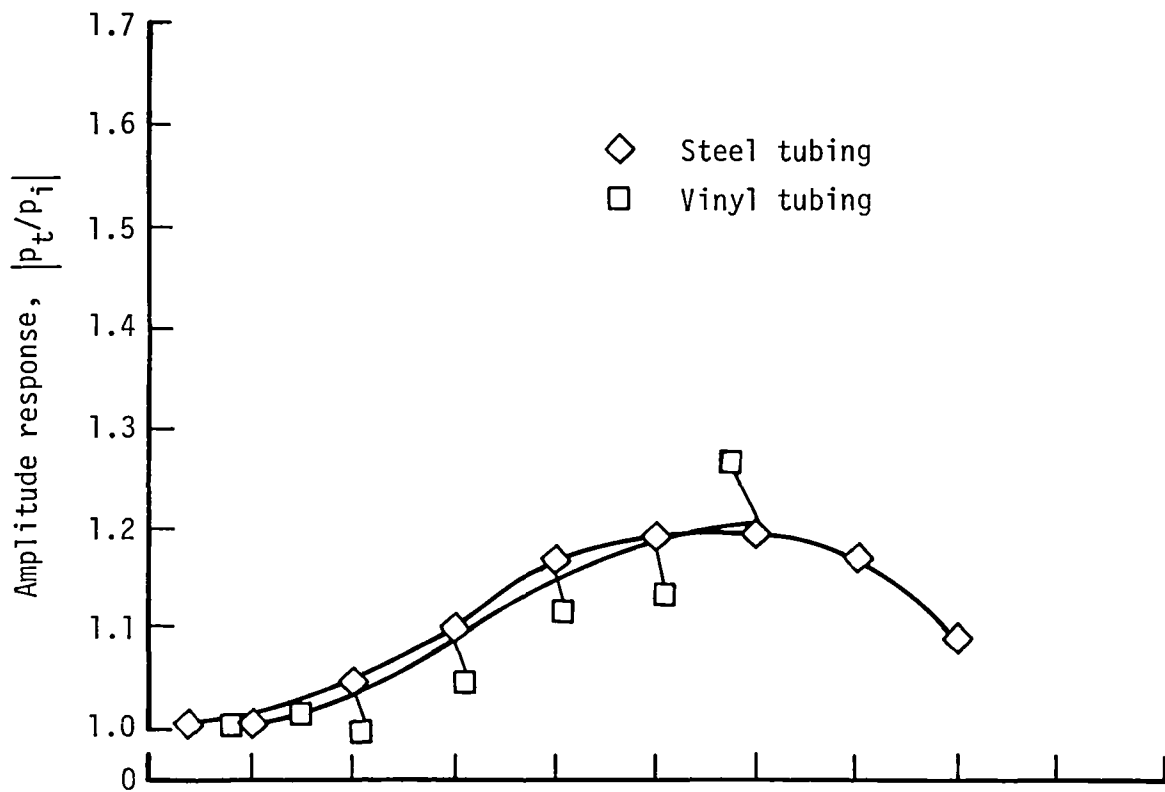


Figure 10.- Sinusoidal response for 0.09-cm inside-diameter vinyl tubing that was 76 cm long.

1. Report No. NASA TM-84650		2. Government Accession No.		3. Recipient's Catalog No.	
4. Title and Subtitle DYNAMIC-PRESSURE MEASUREMENTS USING AN ELECTRONICALLY SCANNED PRESSURE MODULE				5. Report Date July 1983	
				6. Performing Organization Code 505-31-53-09	
7. Author(s) William G. Chapin				8. Performing Organization Report No. L-15583	
9. Performing Organization Name and Address  NASA Langley Research Center Hampton, VA 23665				10. Work Unit No.	
				11. Contract or Grant No.	
12. Sponsoring Agency Name and Address  National Aeronautics and Space Administration Washington, DC 20546				13. Type of Report and Period Covered Technical Memorandum	
				14. Sponsoring Agency Code	
15. Supplementary Notes					
16. Abstract  Frequency response was measured for different lengths and diameters of tubing between a sinusoidal pressure source and a pressure-sensing module from an electronically scanned pressure-measuring system. Measurements were made for straight runs of both steel and vinyl tubing. For steel tubing, measured results are compared with results calculated by using equations developed by Tijdeman and Bergh. Measurements were also made with a bend in the vinyl tubing at the module. In addition, measurements were made with two coils placed in the tubing near the middle of the run.					
17. Key Words (Suggested by Author(s))  Pressure-scanning systems Dynamic-pressure measurement Dynamic-pressure response Pressure-system tubing response			18. Distribution Statement  Unclassified - Unlimited  Subject Category 35		
19. Security Classif. (of this report)  Unclassified		20. Security Classif. (of this page)  Unclassified		21. No. of Pages  22	22. Price  A02



National Aeronautics and  
Space Administration

Washington, D.C.  
20546

Official Business

Penalty for Private Use, \$300

THIRD-CLASS BULK RATE

Postage and Fees Paid  
National Aeronautics and  
Space Administration  
NASA-451



**NASA**

POSTMASTER: If Undeliverable (Section 158  
Postal Manual) Do Not Return

---